[2] A. K. Oki *et al.*, "High performance GaAs/AlGaAs heterojunction bipolar transistor 4-bit and 2-bit A/D converters and 8-bit D/A converter," in *1987 GaAs IC Symp. Tech. Dig.*, pp. 137–140
[3] G M. Gorman, J. B. Camou, A. K. Oki, B. K. Oyama, and M E. Kim, "High performance sample-and-hold implemented with GaAs/AlGaAs heterojunction bipolar transistor technology," in *1987 IEDM Tech. Dig.*, pp 623–626.

Computer-Aided Design of Hybrid and Monolithic Broad-Band Amplifiers for Optoelectronic Receivers

A. PERENNEC, R. SOARES, MEMBER, IEEE, P. JARRY, MEMBER, IEEE, P. LEGAUD, AND M. GOLOUBKOFF, MEMBER, IEEE

Abstract — **In very high data rate fiber-optic systems, it is necessary to have an ultra-wide-band, high-gain, low-noise amplifier after the front end. This paper shows how powerful analytical techniques, such as the real frequency technique, may be applied to the design of a 4 MHz–7 GHz amplifier. A two-stage monolithic amplifier designed according to the theory gives 17 dB gain; a three-stage hybrid amplifier exhibits 16 dB gain across the same frequency band.**

I. Introduction

The real frequency technique [1], [2] has until now been applied to broad-band amplifier design covering two to three octaves. In very high data rate fiber-optic systems, it is necessary to have bandwidth spanning typically three decades. Thus an optical receiver for a 4.8 Gbit/s direct detection system (NRZ code) needs an amplifier with a 6 MHz–6 GHz bandwidth (Fig. 1). Until now, multidecade amplifier design has been largely based upon empirical principles [3]. In this paper, we apply the real frequency technique to the design of a 4 MHz to 7 GHz, 50 Ω amplifier. This method utilizes only the measured scattering parameters of the FET devices. Neither *a priori* knowledge of an equalizer topology nor an analytic form of the system transfer function is assumed. The optimization process of the design procedure is performed simultaneously on the transducer power gain and the *VSWR* using a modified least-squares Marquardt routine which is described by More [4]. Two versions of the amplifier were studied: a two-stage monolithic amplifier realized using the Plessey III–V foundry, and a three-stage hybrid amplifier. The gain, noise figure, and pulse response of each amplifier are presented.

II. Circuit Topology

At low frequencies microwave GaAs MESFET's are unstable and are virtually impossible to match over large bandwidths. This is mainly due to the high input reflection coefficient and the high gain of the device. It is thus necessary to use either lossy matching or *RL* feedback to reduce terminal impedances and stabilize the transistor [3]. A solution integrating both methods has been adopted in our case. The GaAs MESFET is thus embedded in a network including a parallel feedback loop, a drain series inductance, and a gate shunt resistance to form an elementary module termed the transistor feedback block (TFB,

Manuscript received December 3, 1988; revised April 24, 1989
A. Perennec and P. Jarry are with the Laboratoire d'Electronique et Systèmes de Télécommunications, URA CNRS no. 1329, Electronic University, 6 av. Le Gorgeu, 29287 Brest Cedex, France
R. Soares, P. Legaud, and M. Goloubkoff are with CNET—LAB/MER, BP 40, 22301 Lannion Cedex, France.
IEEE Log Number 8928992.

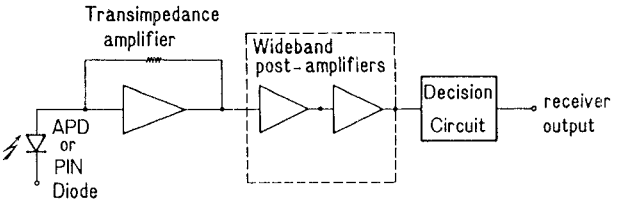

Fig. 1. Fiber-optic system receiver front end.

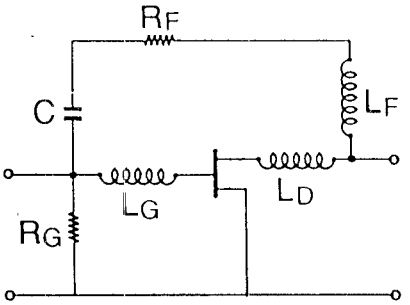

Fig 2 Transistor feedback block (TFB) design.

Fig. 2). This block is designed using the following approach [3]:

- First we choose a value of the feedback resistor, R_F, which gives us a perfect match: $R_F = g_m Z_0^2$.
- But in general $R_F > g_m Z_0^2$; then R_F is made selective by L_F to reduce feedback at higher frequencies. L_D is introduced to compensate for transistor C_{DS}. L_G allows input match and high frequency gain.
- A decoupling capacitor C is introduced into the feedback loop. $C = 50$ pF is a compromise between a high value required to maintain feedback to the lowest frequency possible and minimizing parasitic effects. A damping resistor R_G is introduced to prevent low-frequency oscillations.
- In order to further extend the bandwidth and to improve the gain and *VSWR* performance of the amplifier, the multistage synthesis method outlined in the following section is applied, with the TFB replacing the GaAs MESFET (including also interstage capacitor and bias network) as the active element. Finally the entire TFB is optimized for maximum gain flatness across the widest frequency band.

III. Synthesis Method

The real frequency technique, introduced by Carlin [1], is an optimum approach to broad-band matching. This technique has been extended to double matching and multistage microwave amplifiers [2]. In this section we show how the real frequency technique for multistage matching microwave TFB can be extended to optimize gain and *VSWR*. The optimization is based on a modified least-squares Marquardt routine.

A. The Simplified Real Frequency Technique [2]

In the case of the double matching problem, it has been shown [5] that the scattering parameters of an equalizer, E, can be completely determined from the numerator polynomial $h(p)$ of the input reflection $e_{11}(p)$. E is assumed to be a ladder network; thus the scattering parameters are given as (Belevitch representa-

0018-9480/89/0900-1475$01.00 ©1989 IEEE

tion)

$$e_{11}(p) = h(p)/g(p)$$
$$e_{12}(p) = e_{21}(p) = \pm p^r/g(p)$$
$$e_{22}(p) = -(-1)^r h(-p)/g(p) \quad (1)$$

where $r > 0$ is an integer and specifies the order of the zeros of transmission. In the real frequency technique, the polynomial $h(p) = h_0 + h_1 p + \cdots + h_n p^n$ is chosen as the unknown and the polynomial $g(p)$ is generated from the Hurwitz factorization of

$$g(p)g(-p) = h(p)h(-p) + (-1)^r p^{2r} (E \text{ assumed lossless}). \quad (2)$$

The optimization is performed simultaneously on the transducer power gain and the *VSWR*. In the case of a multistage amplifier the same results are valid.

B. Transducer Power Gain and VSWR

Referring to Fig. 3 for the first k cascaded amplifier stages, the transducer power gain (*TPG*) is given by [2]

$$T_k(\omega) = T_{(k-1)} \frac{|e_{21k}|^2 |S_{21k}|^2}{|1 - e_{11k} S_{Gk}|^2 |1 - \hat{e}_{22k} S_{11k}|^2} \quad (3)$$

i.e.,

$$T_k(\omega) = T_{(k-1)} \cdot E_k(\omega) \quad (4)$$

where T_{k-1} is the *TPG* of the first $(k-1)$ stages with normalized resistive terminations, $(e_{ij})_k$ are the scattering parameters of the kth equalizer E_k, and $(S_{ij})_k$ are the scattering parameters of the kth TFB (F_k).

The overall transducer power gain, $T(\omega)$, is defined after the final equalizer, E_{k+1}, has been added:

$$T(\omega) = (T_1 \cdot T_2 \cdots T_k) E_{(k+1)}(\omega).$$

Using the same method as in [2], we are able to define the *VSWR* of the multistage microwave TFB amplifier. Due to the optimization technique, the input *VSWR* must be defined including all the stages of the amplifier. For the first k cascades stages, the input *VSWR* is given by [6]–[9]

$$R_{\text{in}\,k} = \left. \frac{1 + |\hat{e}_{11\,1}|}{1 - |\hat{e}_{11\,1}|} \right|_k. \quad (5)$$

Due to the optimization technique, the overall output *VSWR* is only defined after the final equalizer, E_{k+1}, has been added:

$$R_{\text{out}} = \frac{1 + |\hat{e}_{22(k+1)}|}{1 - |\hat{e}_{22(k+1)}|}. \quad (6)$$

C. Optimization of Gain and VSWR

Optimization is performed simultaneously upon the transducer power gain and the *VSWR* as follows [6], [9], [10]:

1) First construct the input equalizer E_1 such that $T_1(\omega) = E_1(\omega)$ and the input *VSWR* ($R_{\text{in}\,1}$) are optimized. The approach is formulated by using a least-squares method. The objective function may be written as

$$E = \sum_{j=1}^{m} W_1 \left(T_1(\omega_j)/T_{10} - 1 \right)^2 + W_2 \left(R_{\text{in}\,1}(\omega_j)/R_{\text{in}\,0} - 1 \right)^2 \quad (7)$$

where T_{10} and $R_{\text{in}\,0}$ are the desired gain and input *VSWR* to be approximated in the least-squares sense, m is the number of sampling frequencies over the passband, and W_1 and W_2 are weighting functions. At each iteration, coefficients $h_i + \Delta h_i$ are corrected to minimize the objective function using the Levenberg–Marquardt algorithm. Vector $\Delta \boldsymbol{h}$ is given as

$$\Delta \boldsymbol{h} = -\left[\boldsymbol{J}^T \boldsymbol{J} + \alpha \boldsymbol{D}^T \boldsymbol{D} \right]^{-1} \boldsymbol{J}^T \boldsymbol{e}_0 \quad (8)$$

where $\boldsymbol{e}_0$ is the initial error vector, $\boldsymbol{J}$ is the Jacobian matrix of $\boldsymbol{e}$ (where the elements are: $\partial e_j / \partial h_i$; $j = 1 \cdots m$; $i = 1 \cdots n$), $\boldsymbol{D}$ is a diagonal matrix, and α is the Levenberg–Marquardt parameter. More [4] introduced relationships between $\boldsymbol{J}$, $\boldsymbol{D}$, and α which permit rapid convergence.

2) The second stage (equalizer E_2 and TFB) is now cascaded and computed so that $T_2(\omega) = T_1 E_2(\omega)$ and $R_{\text{in}\,2}$ are optimized. T_1 is known from the first stage and is now a weighting factor.

3) The remaining stages are all cascaded to provide good optimizations on gain and input *VSWR*. Only the final equalizer, E_{k+1}, will be used to obtain a good approximation of the output *VSWR*.

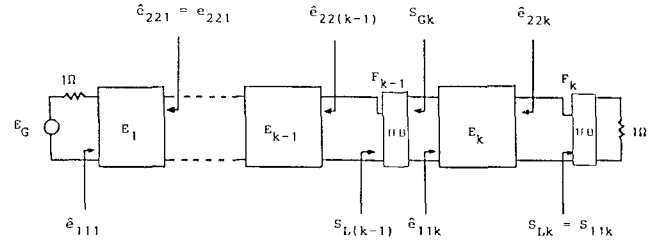

Fig. 3 Computation steps for designing a broad-band multistage microwave FET amplifier.

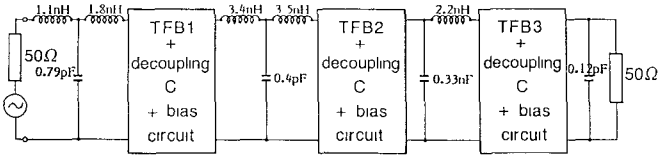

Fig. 4 Broad-band 4 MHz to 6 GHz three-stage GaAs FET gain block.

D. Hybrid Realization [9], [10]

The real frequency technique has been applied to the design of a 4 MHz to 6 GHz amplifier for a wide-band fiber-optic receiver. The amplifier design makes use of frequency-controlled feedback, and the circuit topology for the matching networks has been resolved by using the real frequency method. The technique results in element values which are convenient to realize, as may be seen by inspection of Fig. 4.

A hybrid 4 MHz to 6 GHz amplifier has been produced using three RTC-CFX 31X GaAs FET's at CNET Lannion (France). Only the drain was supplied with current at 4 V, the gate being grounded via a shunt resistor R_G (see Fig. 2). Implementation was made on a 0.635-mm-thick alumina substrate. Lumped capacitors were made with layered ceramics, and inductors were realized by gold wires.

Fig. 5 shows the hybrid implementation of the three-stage amplifier fabricated on a 1 inch square alumina substrate.

The measured performance of this amplifier is shown in Fig. 6 together with the theoretical gain and *VSWR*. The small-signal gain is 16 dB with a good flatness (± 1 dB) across the 4 MHz to 6 GHz frequency range. Input and output *VSWR*'s are less than 3:1. One dB gain compression was measured as 9 dBm at 2 GHz and 6 GHz, and a noise figure less than 9 dB was obtained, apart from a local peak at 4 GHz.

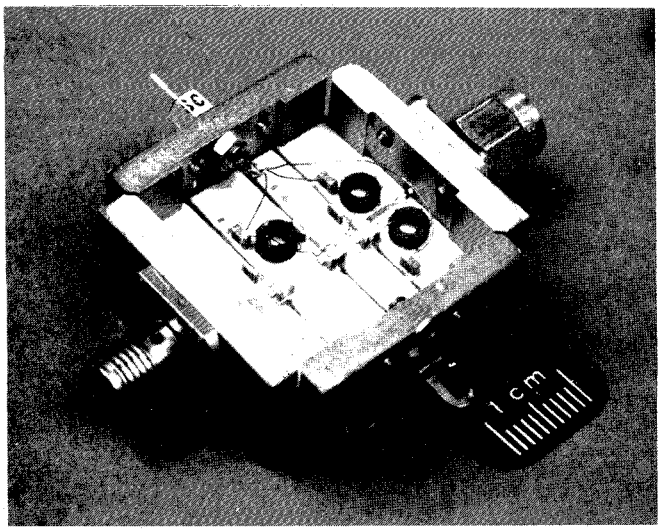

Fig. 5. Hybrid three-stage 4 MHz to 6 GHz FET amplifier.

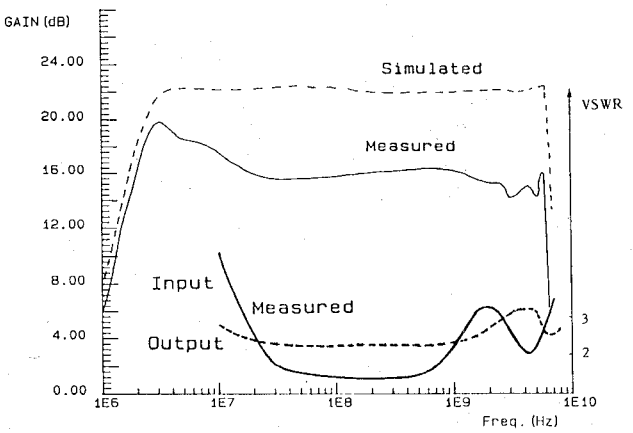

Fig. 6. Gain and *VSWR* performances of 4 MHz to 6 GHz hybrid FET amplifier.

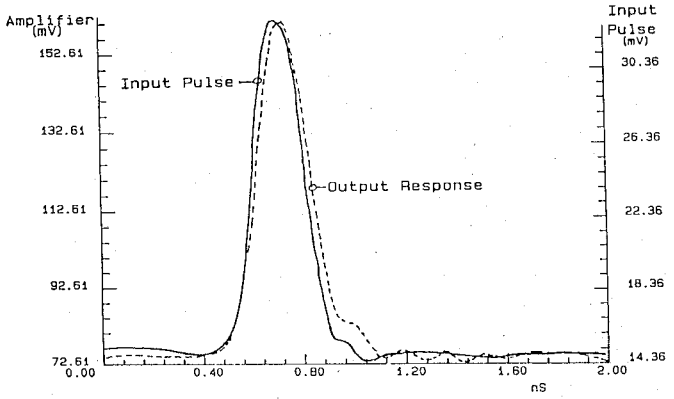

Fig. 7. For a 5 Gbit/s impulse: impulse and amplifier output responses superimposed.

Fig. 7 presents the response of this hybrid amplifier to a 5 Gbit/s pulse. We observe that the distortion is negligible. This example shows that the matching equalizers obtained by the real frequency technique are realizable. It should be noted that the nonunilateral behavior of the TFB has been taken into account. Our experimental results are in good agreement with the theoretical calculation.

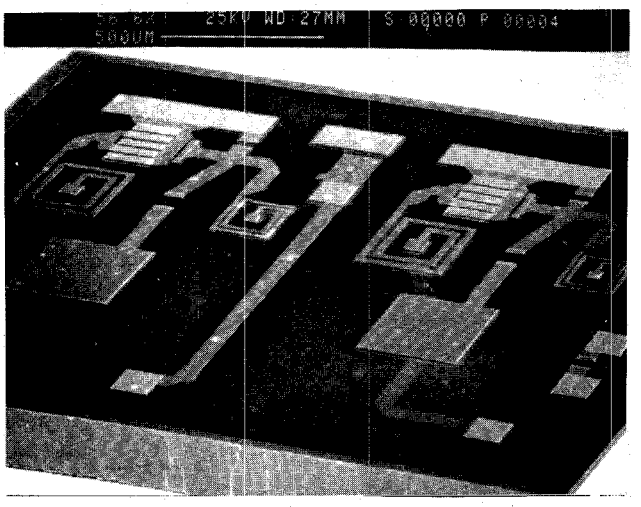

Fig. 8. Monolithic realization.

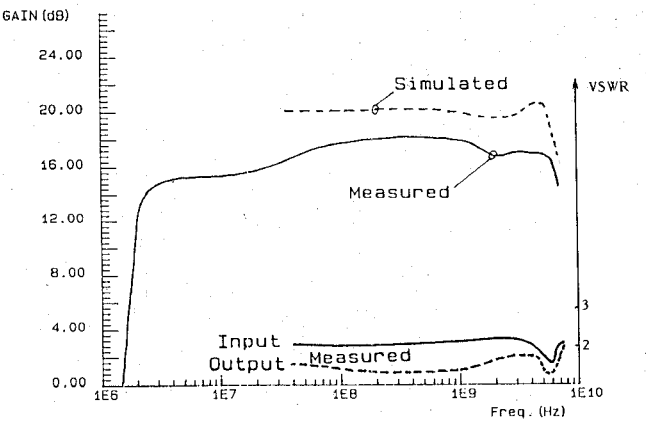

Fig. 9. Gain and *VSWR* performances of the two-stage monolithic amplifier.

E. Monolithic Realization [9], [10]

The monolithic version of the amplifier was realized using the Plessey III–V foundry on a multichip project. The chip size was 2.3 mm×1.8 mm. The chip area used was optimized by incorporating two independent amplifier stages. The amplifiers are identical, apart from input and output locations, which are necessarily different to enable each amplifier stage to be used independently *or* to enable the two to be cascaded via an external off-chip capacitor.

A photomicrograph of the chip is given in Fig. 8. The transistor drains are biased via the RF output lead from each stage, the gates being grounded via the shunt resistor, as in the hybrid case. The performance of the two-stage monolithic amplifier mounted in a miniaturized hybrid alumina substrate, and incorporating ferrite bead RF chokes in the bias circuit, is given in Fig. 9. The gain is 17 dB ±1 dB and input and output *VSWR*'s are less than 2:1 over the 5 MHz to 7 GHz frequency range. Noise figure above 200 MHz is less than 5.5 dB and a 1 dB gain compression point greater than 18 dBm has been measured at several discrete frequencies.

IV. Conclusion

The simplified real frequency synthesis technique has been adapted to the design of a 5 MHz to 6 GHz ultra-broad-band amplifier. A three-stage hybrid amplifier and a two-stage mono-

lithic amplifier have been realized using the theory. The results obtained confirm the value of the synthesis approach used. The amplifiers are to be used for optical detection at very high data rates.

References

[1] H J Carlin, "A new approach to gain–bandwidth problems," *IEEE Trans Circuits Syst*, vol CAS-23, pp 170–175, Apr. 1977

[2] B S Yarman and H J. Carlin, "A simplified 'real frequency' technique applied to broad-band multistage microwave amplifiers," *IEEE Trans Microwave Theory Tech.*, vol. MTT-30, pp. 2216–2222, Dec 1982.

[3] R Wroblenski, *GaAs MESFET Circuit Design*, R Soares, Ed. Norwood, MA: Artech House, 1988, ch 3

[4] J. J More, "The Levenberg–Marquardt algorithm· Implementation and theory," Lecture notes in Mathematics 630, Springer-Verlag, 1978.

[5] V Belevitch, "Elementary application of the scattering formalism to network design," *IRE Trans Circuit Theory*, vol CT-3, June 1956

[6] P. Jarry and A Perennec, "Optimization of gain and VSWR in multistage microwave amplifier using the real frequency method," in *Proc ECCTD'87* (Paris), 1–4 Sept 1987, pp 203–208.

[7] A. Perennec and P Jarry, "Real frequency broadband microwave matching using a modified Marquardt optimization," in *Proc IEEE Melecon 87* (Rome), Mar. 1987, pp. 319–322

[8] P Jarry, A. Perennec, and J. Le Bihan, "Optimisation et synthèse d'amplificateurs microondes par la méthode des fréquences réelles," *Rev Phys. Appl*, pp. 137–142, Feb. 1988

[9] A Perennec, "Synthèse et réalisations d'amplificateurs microondes par la méthode des fréquences réelles," Thèse nouveau régime Electronique, Université de Brest, July 1988.

[10] A. Perennec, R Soares, P Jarry, P Legaud, and R. Boitin, "Application of Circuit Synthesis to the design of a three-stage 4 MHz to 7 GHz amplifier for a wide band fiber optics receiver," presented at 18th European Microwave Conf, Stockholm, Sept 1988.

Output Conductance Frequency Dispersion and Low-Frequency Noise in HEMT's and MESFET's

J. A. REYNOSO-HERNANDEZ AND J. GRAFFEUIL,
ASSOCIATE MEMBER, IEEE

Abstract—**In this paper it is reported that the large low-frequency noise observed in MESFET's and HEMT's in the saturation regime usually scales with the device output conductance frequency dispersion (in MESFET's) or with the parallel conduction through the GaAlAs (in HEMT's).**

I. Introduction

Both GaAs MESFET's and HEMT's exhibit a large low-frequency noise, which severely limits the possible applications of these devices for wide-band and dc coupled amplifiers, digital analog converters, low-noise oscillators, and mixers [1]–[4].

On the other hand, frequency dispersion of the output conductance of MESFET's [5] is a serious problem for the design of analog circuits such as power amplifiers and certain digital circuits [6].

Manuscript received December 12, 1988: revised April 20, 1989. This work was supported in part by the Centre National D'Etudes Spatiales (CNES) and by the Mexican government under Grant CONACYT (Mexico).

J. A Reynoso-Hernandez is with the Laboratoire D'Automatique et D'Analyse des Systèmes du C.N.R.S, 7, Avenue du Colonel Roche, 31400 Toulouse, France

J Graffeuil is with the Laboratoire D'Automatique et D'Analyse des Systèmes du C.N.R.S, 7, Avenue du Colonel Roche, 31400 Toulouse, France, and with the Université Paul Sabatier de Toulouse, 118 Route de Narbonne, 31078 Toulouse, France.

IEEE Log Number 8928996

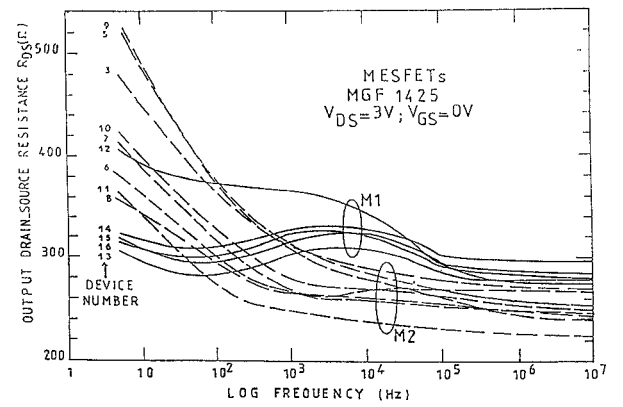

(a)

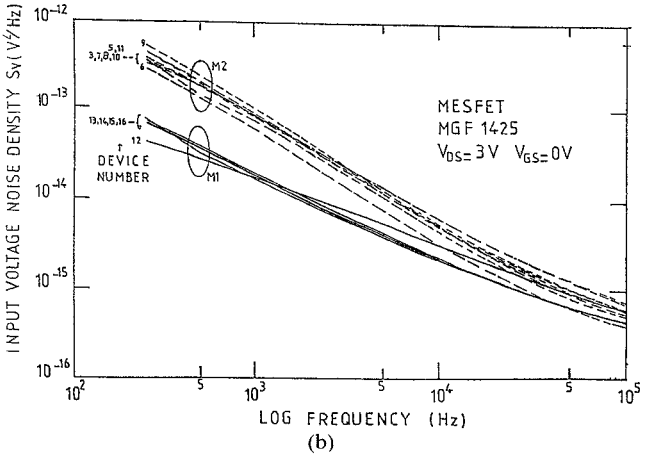

(b)

Fig. 1 (a) Frequency dependence of small-signal output drain–source resistance for a set of 13 MESFET's measured in saturation regime at $V_{ds} = 3$ V and $V_{gs} = 0$ V. (b) Spectral noise input voltage for the set of 13 MESFET's measured in saturation regime at $V_{ds} = 3$ V and $V_{gs} = 0$ V.

It has been proposed recently [7] that deep levels of this type can cause low-frequency noise and output conductance frequency dispersion. The present paper first experimentally investigates whether such a correlation between LF noise and conductance dispersion can be observed among some commercially available MESFET's. Second, this paper investigates whether commercially available HEMT's exhibit a similar behavior.

II. Measurements

We have investigated simultaneously a set of 13 commercially available MESFET's (MITSUBISHI MGF 1425) and a set of ten commercially available HEMT's (MITSUBISHI MGF 4303). We have successively performed room-temperature measurements on each device concerning a) the low-frequency input voltage noise spectral density between 250 Hz and 100 kHz, b) frequency dispersion of the output drain-source impedance $Z_d(f)$ in the frequency range 5 Hz–10 MHz, and c) static g_m variations versus gate bias. The drain bias was fixed at 3 V (MESFET) and 2 V (HEMT), and the gate bias was taken to be zero for the first and second sets of measurements.

All measurements were controlled and corrected by software. The noise measurement system has been reported elsewhere [4].